



*Supplement of*

## **Processes driving the regional sensitivities of summertime $\text{PM}_{2.5}$ to temperature across the US: new insights from model simulations**

**Lifei Yin et al.**

*Correspondence to:* Pengfei Liu ([pengfei.liu@eas.gatech.edu](mailto:pengfei.liu@eas.gatech.edu))

The copyright of individual parts of the supplement might differ from the article licence.

**Figure S1.** The categorization of four subregions of the contiguous United States used in this study.

**Figure S2.** Same as Figure 1 a1-a5 in the main text but displaying only temperature sensitivities that are statistically significant ( $p < 0.05$ ).

**Figure S3.** Spatial distribution of average summer concentrations of PM<sub>2.5</sub> and its species derived from ground-based observations and four GEOS-Chem simulation cases. Panels (a1–f1) show the concentrations of PM<sub>2.5</sub> (a1–a5), organic aerosol (OA) (b1–b5), sulfate (c1–c5), nitrate (d1–d5), ammonium (e1–e5), and black carbon (BC) (f1–f5) for REF\_2019 case (2000-2017 average), MAIN\_HighRes case (2000-2022 average), MAIN\_LowRes case (2000-2022 average), and MAIN\_LowRes\_SimpSOA case (2000-2017 average). Detailed descriptions of the GEOS-Chem simulation cases are provided in Table 1 of the main text.

**Figure S4.** Time series of regional average concentrations derived from ground-based observations, machine-learning-modeled data, and four GEOS-Chem simulation cases. Panels (a1–f1) show the concentrations of PM<sub>2.5</sub> (a1–a5), organic aerosol (OA) (b1–b5), sulfate (c1–c5), nitrate (d1–d5), ammonium (e1–e5), and black carbon (BC) (f1–f5) for the contiguous US (a1–f1), Southeast US (a2–f2), Northeast US (a3–f3), West US (a4–f4), and Central US (a5–f5).

**Figure S5.** NH<sub>3</sub> emissions during summer months (June, July, August) from the NEI 2011 inventory and the NEI 2016 inventory for the contiguous United States (a) and the Southeast US (b).

**Figure S6** Sensitivities of surface concentration to summer mean temperature anomalies for five major components of PM<sub>2.5</sub> derived from four GEOS-Chem cases and ground-based observations from 2000-2016. Triangle markers represent fitted slopes (sensitivities) with  $p < 0.05$ . a-e, temperature sensitivity of summertime organic aerosols (OA) (a1-a4), sulfate (b1-b4), ammonium (c1-c4), nitrate (d1-d4), and elemental carbon (EC) (e1-e4) simulated by REF\_2019 case, MAIN\_HighRes case, MAIN\_LowRes case, and MAIN\_LowRes\_SimpSOA case. Please refer to Table 1 in the main text for details on the GEOS-Chem cases.

**Figure S7** Regional sensitivities of surface concentration to summer mean temperature anomalies five major components of PM<sub>2.5</sub> derived from four GEOS-Chem cases and ground-based observations from 2000-2016. a-e, temperature sensitivity of organic aerosols (OA), sulfate, ammonium, nitrate, and elemental carbon (EC). For each region, the bars (from left to right) represent results from observations (OBS), REF\_2019 case, MAIN\_HighRes case, MAIN\_LowRes case, and MAIN\_LowRes\_SimpSOA case. Detailed descriptions of the GEOS-Chem simulation cases are provided in Table 1 of the main text.

**Figure S8.** Daytime slopes of monthly mean cloud fractions in the lower troposphere (> 680 hPa) versus surface air temperature over land for June–July–August during 2000–2022, based on MERRA2 meteorology. White areas indicate slopes that are not statistically significant at the 0.05 level.

**Figure S9.** Annual scaling factors for SO<sub>2</sub> emissions from energy generation units, derived from the NEI inventory and raw CAMD data.

**Figure S10.** CAMD-derived scaling factors for SO<sub>2</sub> emissions (a) and NO<sub>x</sub> emissions (b) from energy generation units during summer months.

**Figure S11.** Coefficient of determination ( $r^2$ ) and root-mean-square error (RMSE) between observations and four GEOS-Chem cases for PM<sub>2.5</sub> and its five major components. Panels (a1–f1) show the  $r^2$  values for PM<sub>2.5</sub>, organic aerosols (OA), sulfate, ammonium, nitrate, and black carbon (BC), respectively. Panels (a1–f1) show the corresponding RMSE values for the same species.

**Figure S12.** Same as Figure 2 in the main text, but for ammonium, nitrate, and black carbon (BC).

**Figure S13.** Regional-aggregated temperature sensitivity of PM<sub>2.5</sub> for 10-year running time windows, derived from ground-based observations and MAIN\_HighRes case. The shaded areas represent the 95% confidence interval across each region.

**Figure S14.** Regional-aggregated temperature sensitivity of three major organic aerosol (OA) species from four GEOS-Chem cases. Panels a1-a5 shows the temperature sensitivity of primary OA for the contiguous US (a1), the Southeast US (a2), the Northeast US (a3), the West US (a4), and the Central US (a5); Panels b1-b5 shows the temperature sensitivity of aqueous-phase formed isoprene OA (ISOAAQ) for each region; Panels c1-c5 shows the temperature sensitivity of monoterpene SOA (TSOA) for each region. The MAIN\_LowRes\_SimpSOA case reports total SOA concentrations as a single variable SOAS, which is shown with ISOAAQ in panels b1-b5.

**Figure S15.** Budget diagnostic for aqueous-phase-formed isoprene SOA (ISOAAQ) simulated by the MAIN\_HighRes case and the temperature sensitivity of each process. Panels (a1–d1) show the budget diagnostic for transport (a1), mixing (b1), wet deposition (c1), and convention (d1) process and the corresponding temperature sensitivity (a2-d2).

**Figure S16.** Same as Figure S15 but for sulfate budget diagnostic.

**Figure S17.** Time series for budget diagnostic and efficiency of driving processes of ISOAAQ concentration. Panels a1-a5 shows the time series for budget diagnostic for the contiguous US (a1), the Southeast US (a2), the Northeast US (a3), the West US (a4), and the Central US (a5); Panels b1-b5 shows the time series for removal efficiency for each region.

**Figure S18.** Same as Figure S17 but for sulfate budget diagnostic.

**Figure S19.** Same as Figure 5 in the main text but for primary organic aerosol (POA) and secondary organic aerosol formed from monoterpene oxidation (TSOA).

**Figure S20.** Production rate (a1-a3) and corresponding temperature sensitivity (b1-b3) of three major sulfate production processes. Panels c1-c5 shows the time series for temperature sensitivity of each pathway for the contiguous US (a1), the Southeast US (a2), the Northeast US (a3), the West US (a4), and the Central US (a5).

**Figure S21.** Contributions from isoprene-mediated and sulfate-mediated processes to the overall temperature sensitivity of isoprene SOA (ISOAAQ). The shading areas represent 95%

confidence interval. Panels a1-a5 show the time series of isoprene-mediated process breakdown for the contiguous US (a1), Southeast US (a2), Northeast US (a3), West US (a4), and Central US (a5); Panels b1-b5 show the time series of sulfate-mediated process breakdown for each region. Please refer to Eq. (1) in the main text for detailed expression.

**Figure S22.** Same as Figure S21 but for sulfate. Please refer to Eq. (2) in the main text for detailed expression.

**Figure S23.** Same as Figure S21 but for monoterpene SOA (TSOA). Please refer to Eq. (3) in the main text for detailed expression.

**Figure S24.** Same as Figure 6 a, b in the main text but for 3-year rolling window.

**Figure S25.** Same as Figure 6 in the main text but for nitrate aerosol. Please refer to Eq. (4) in the main text for detailed expression.

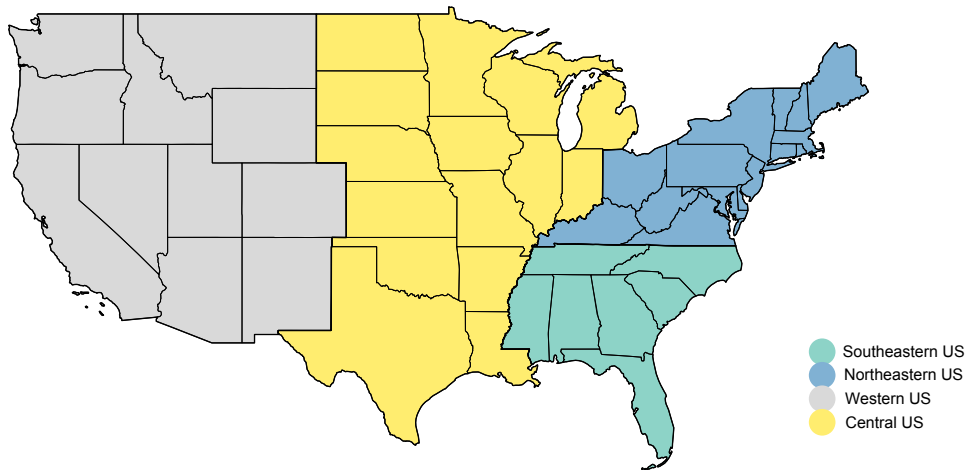


**Figure S1.** The categorization of four subregions of the contiguous United States used in this study.

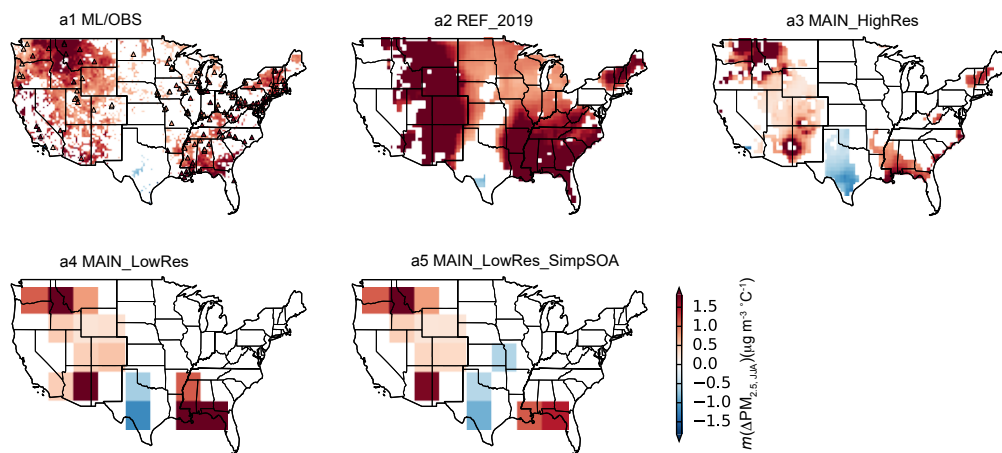


**Figure S2.** Same as Figure 1 a1-a5 in the main text but displaying only temperature sensitivities that are statistically significant ( $p < 0.05$ ).

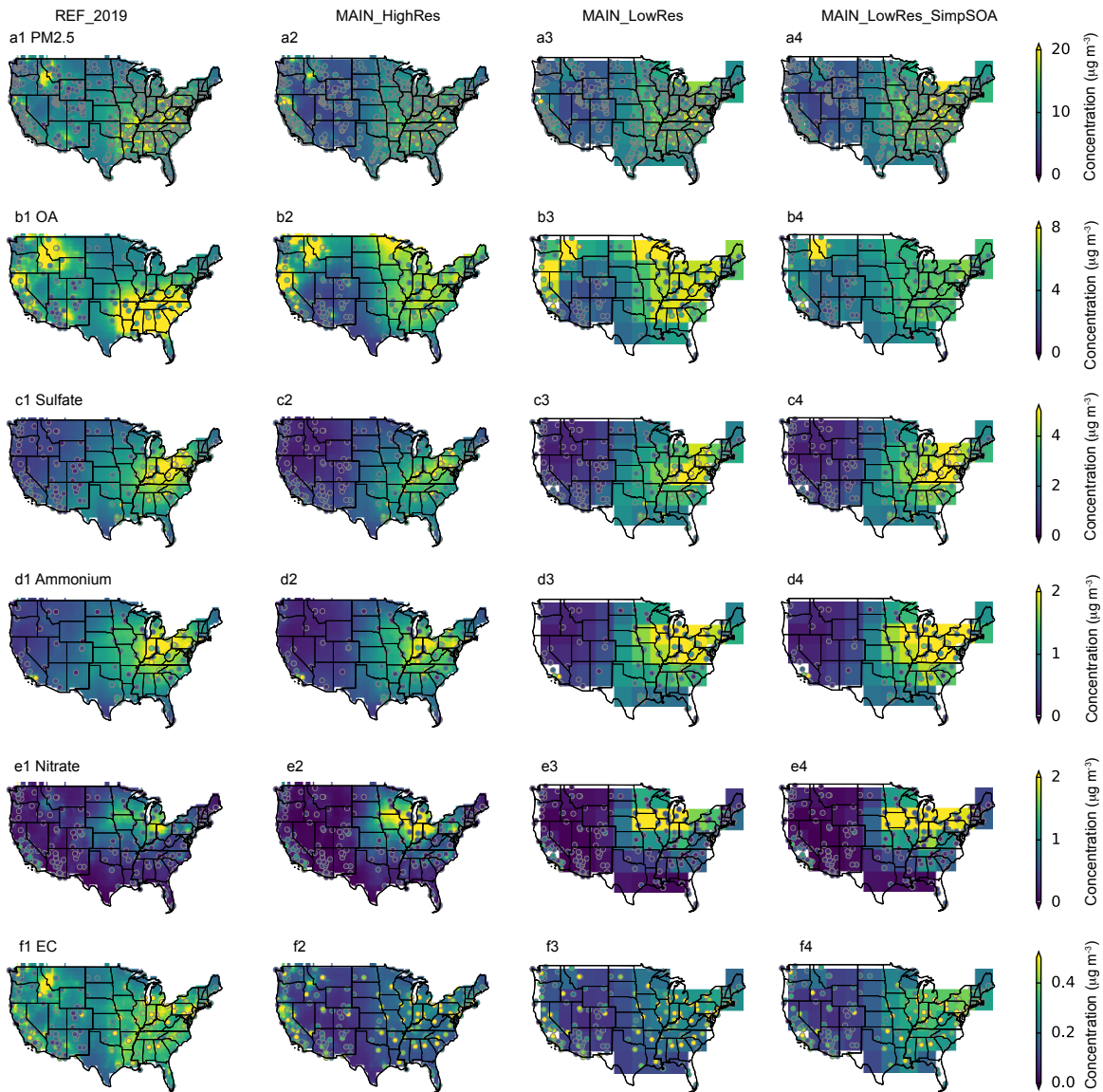


**Figure S3.** Spatial distribution of average summer concentrations of  $PM_{2.5}$  and its species derived from ground-based observations and four GEOS-Chem simulation cases. Panels (a1–f1) show the concentrations of  $PM_{2.5}$  (a1–a5), organic aerosol (OA) (b1–b5), sulfate (c1–c5), nitrate (d1–d5), ammonium (e1–e5), and black carbon (BC) (f1–f5) for REF\_2019 case (2000–2017 average), MAIN\_HighRes case (2000–2022 average), MAIN\_LowRes case (2000–2022 average), and MAIN\_LowRes\_SimpSOA case (2000–2017 average). Detailed descriptions of the GEOS-Chem simulation cases are provided in Table 1 of the main text.

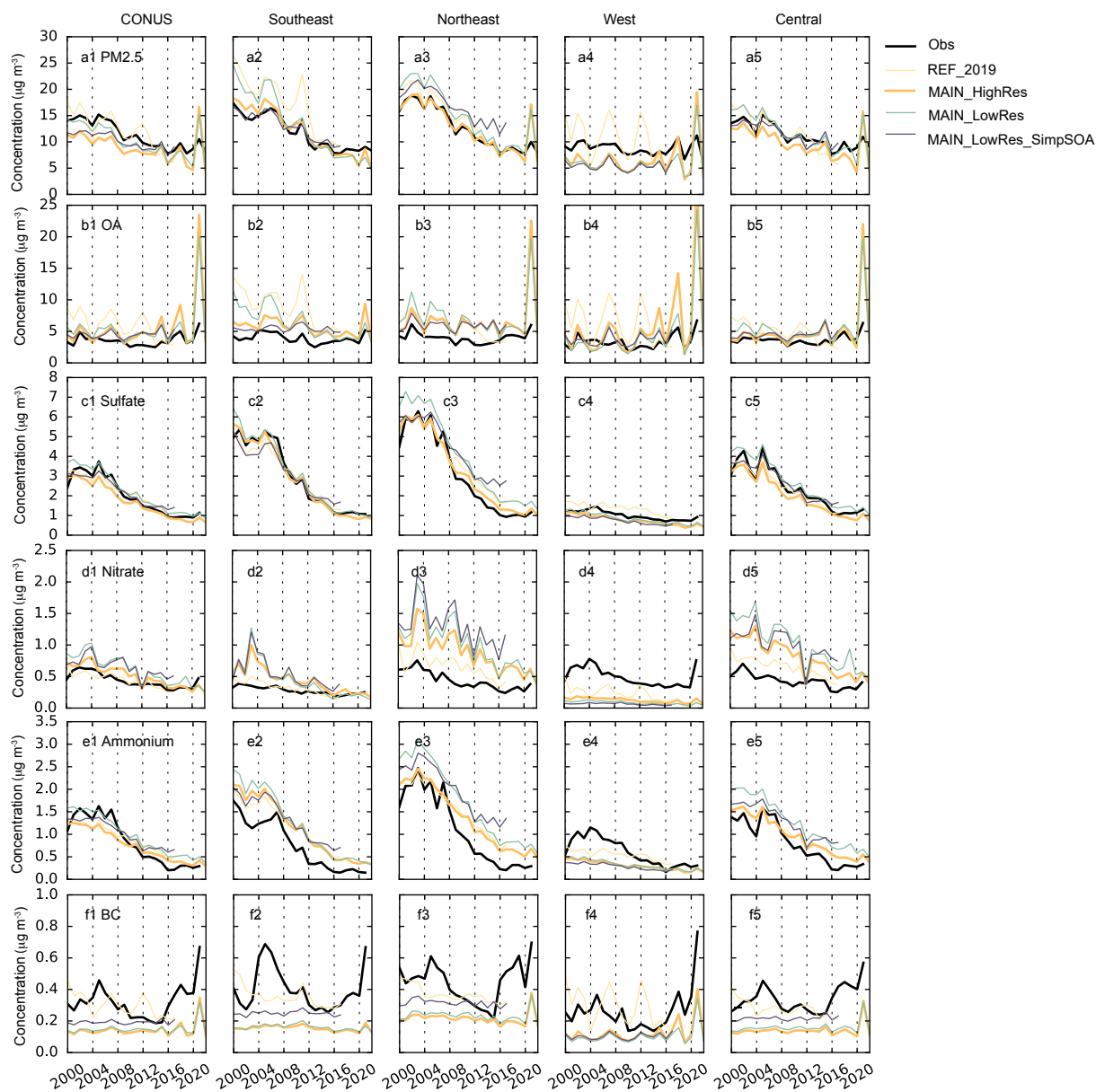


**Figure S4.** Time series of regional average concentrations derived from ground-based observations, machine-learning-modeled data, and four GEOS-Chem simulation cases. Panels (a1–f1) show the concentrations of  $PM_{2.5}$  (a1–a5), organic aerosol (OA) (b1–b5), sulfate (c1–c5), nitrate (d1–d5), ammonium (e1–e5), and black carbon (BC) (f1–f5) for the contiguous US (a1–f1), Southeast US (a2–f2), Northeast US (a3–f3), West US (a4–f4), and Central US (a5–f5).

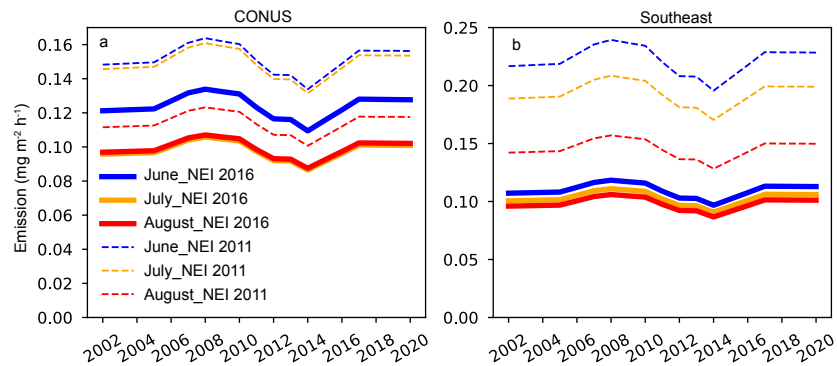


**Figure S5.** NH<sub>3</sub> emissions during summer months (June, July, August) from the NEI 2011 inventory and the NEI 2016 inventory for the contiguous United States (a) and the Southeast US (b).

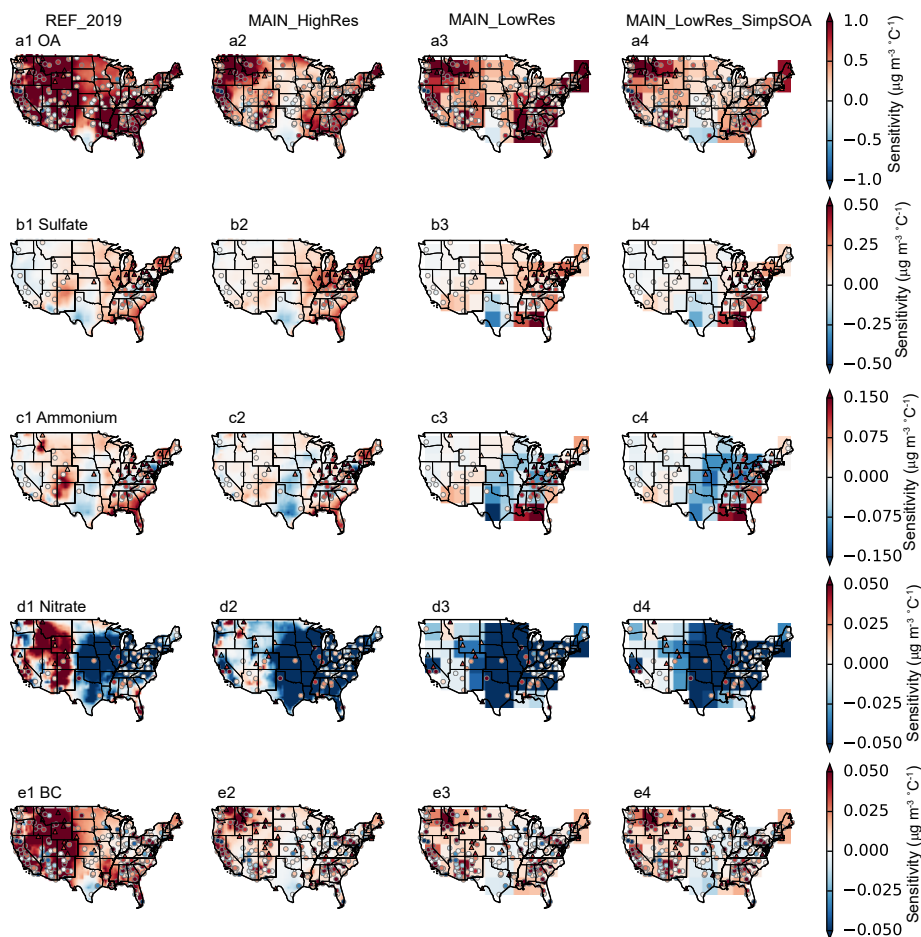


**Figure S6.** Sensitivities of surface concentration to summer mean temperature anomalies for five major components of  $PM_{2.5}$  derived from four GEOS-Chem cases and ground-based observations. Triangle markers represent fitted slopes (sensitivities) with  $p < 0.05$ . a-e, temperature sensitivity of summertime organic aerosols (OA) (a1-a4), sulfate (b1-b4), ammonium (c1-c4), nitrate (d1-d4), and elemental carbon (EC) (e1-e4) simulated by REF\_2019 case, MAIN\_HighRes case, MAIN\_LowRes case, and MAIN\_LowRes\_SimpSOA case. Please refer to Table 1 in the main text for details on the GEOS-Chem cases.

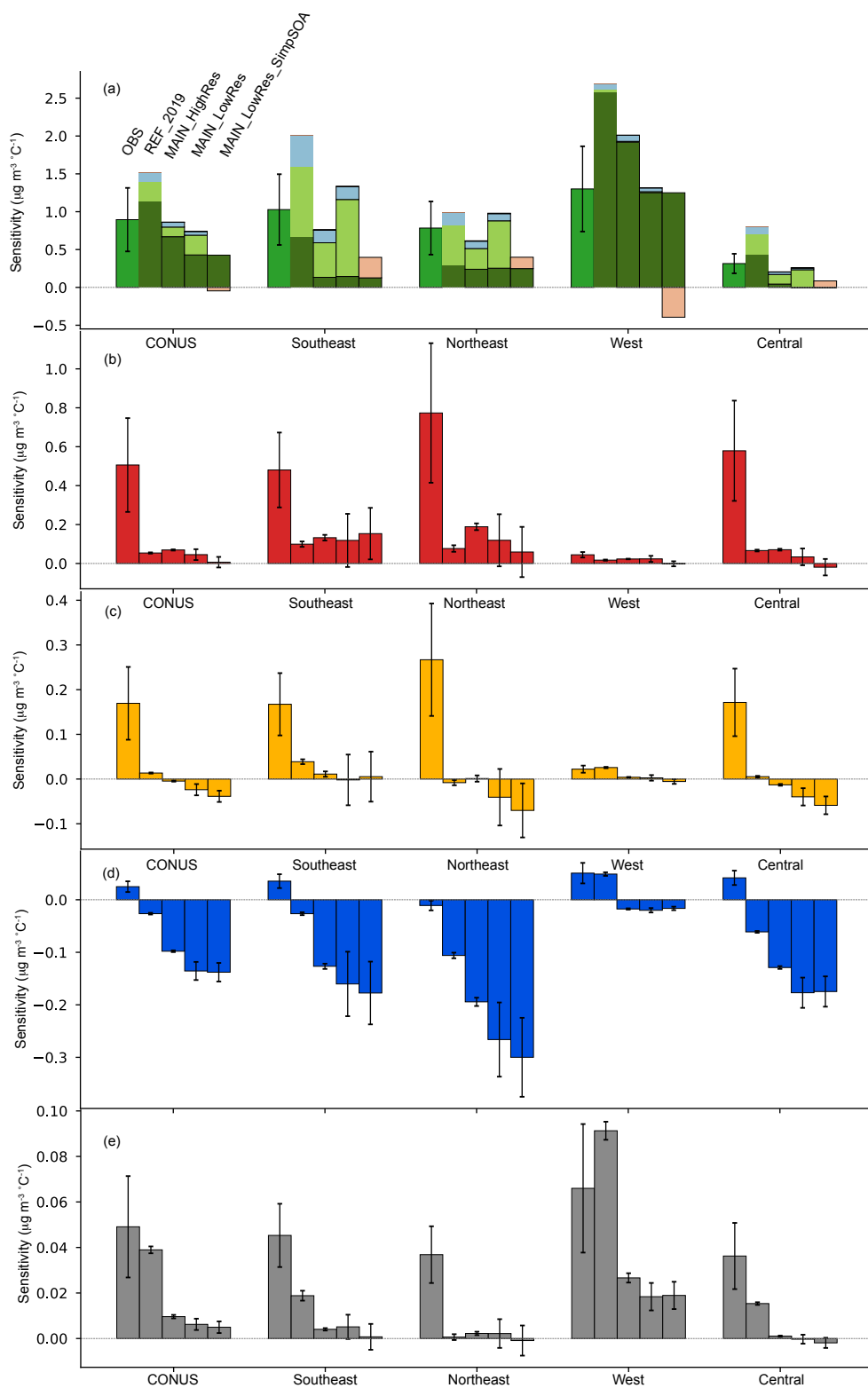


**Figure S7.** Regional sensitivities of surface concentration to summer mean temperature anomalies five major components of PM<sub>2.5</sub> derived from four GEOS-Chem cases and ground-based observations from 2000-2016. a-e, temperature sensitivity of organic aerosols (OA), sulfate, ammonium, nitrate, and elemental carbon (EC). For each region, the bars (from left to right) represent results from observations (OBS), REF\_2019 case, MAIN\_HighRes case, MAIN\_LowRes case, and MAIN\_LowRes\_SimpSOA case. Detailed descriptions of the GEOS-Chem simulation cases are provided in Table 1 of the main text.

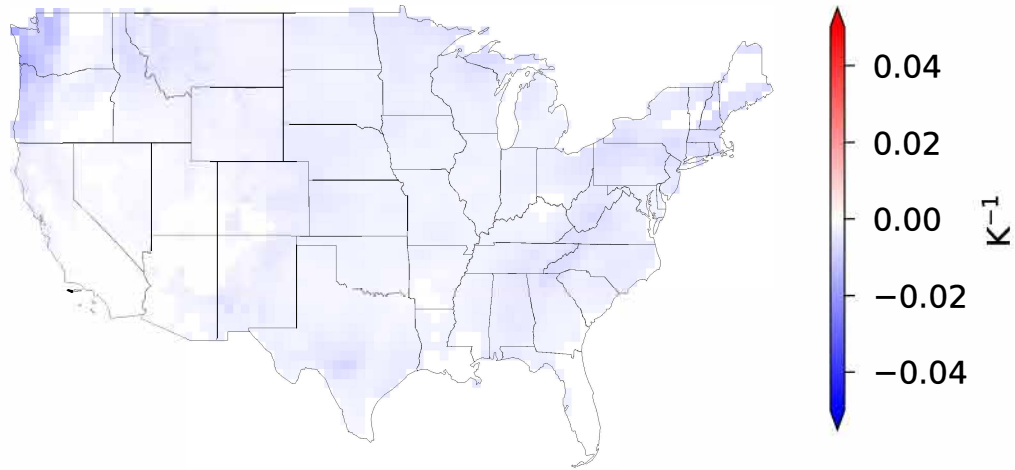


**Figure S8.** Daytime slopes of monthly mean cloud fractions in the lower troposphere (> 680 hPa) versus surface air temperature over land for June–July–August during 2000–2022, based on MERRA2 meteorology. White areas indicate slopes that are not statistically significant at the 0.05 level.

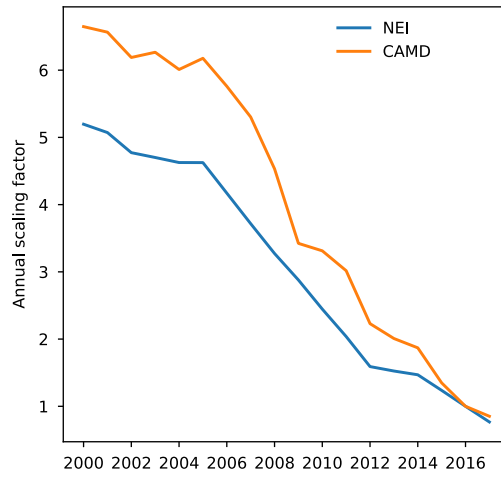


**Figure S9.** Annual scaling factors for SO<sub>2</sub> emissions from energy generation units, derived from the NEI inventory and raw CAMD data.

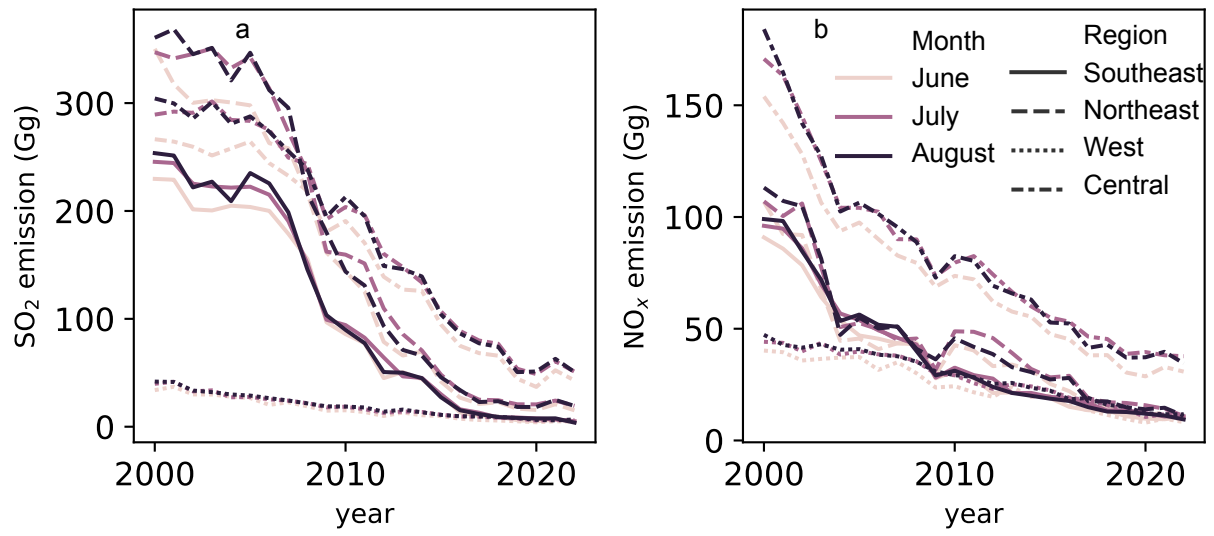


**Figure S10.** CAMD-derived scaling factors for SO<sub>2</sub> emissions (a) and NO<sub>x</sub> emissions (b) from energy generation units during summer months.

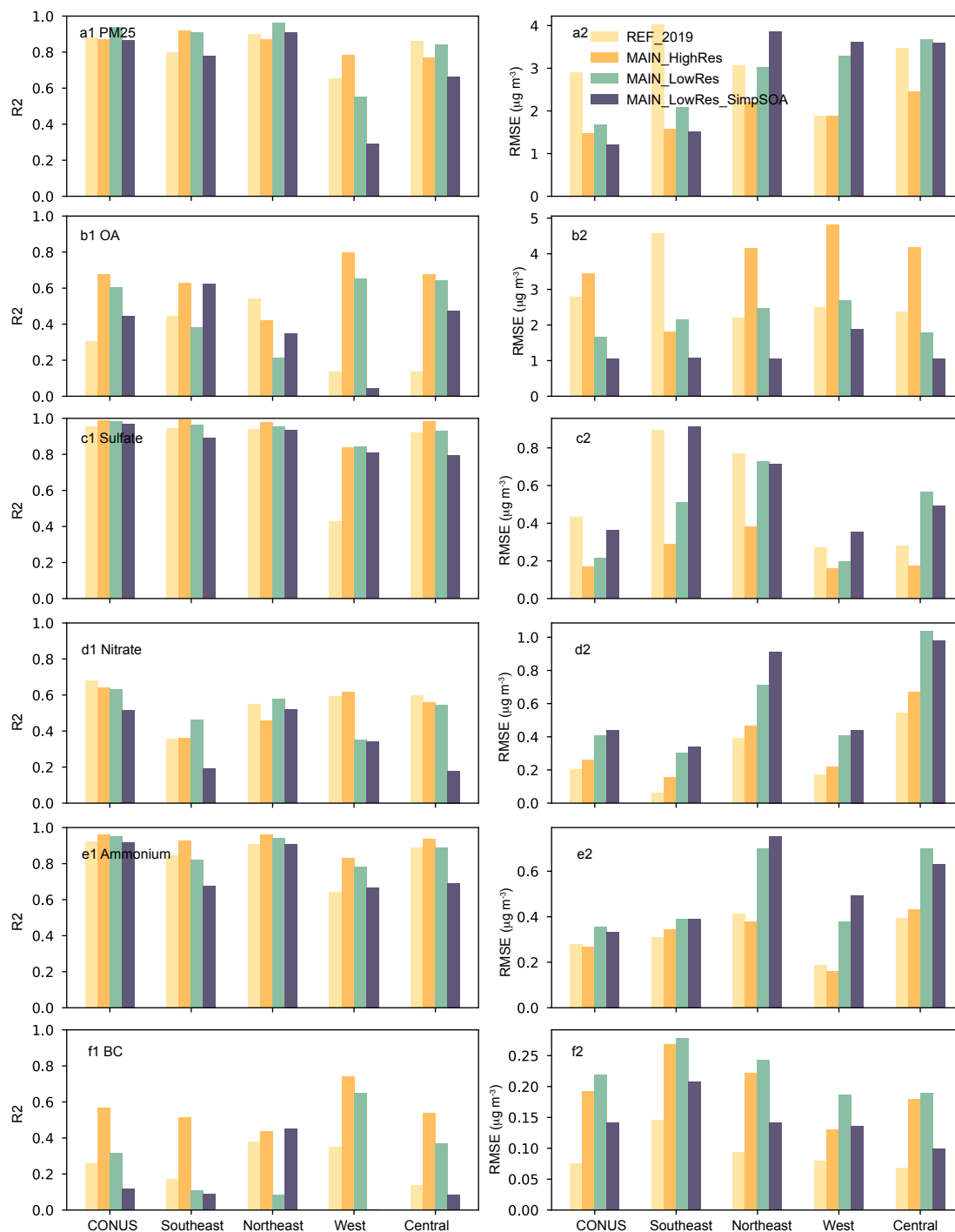


**Figure S11.** Coefficient of determination ( $r^2$ ) and root-mean-square error (RMSE) between observations and four GEOS-Chem cases for concentration of PM<sub>2.5</sub> and its five major components. Panels (a1–f1) show the  $r^2$  values for PM<sub>2.5</sub>, organic aerosols (OA), sulfate, ammonium, nitrate, and black carbon (BC), respectively. Panels (a1–f1) show the corresponding RMSE values for the same species.

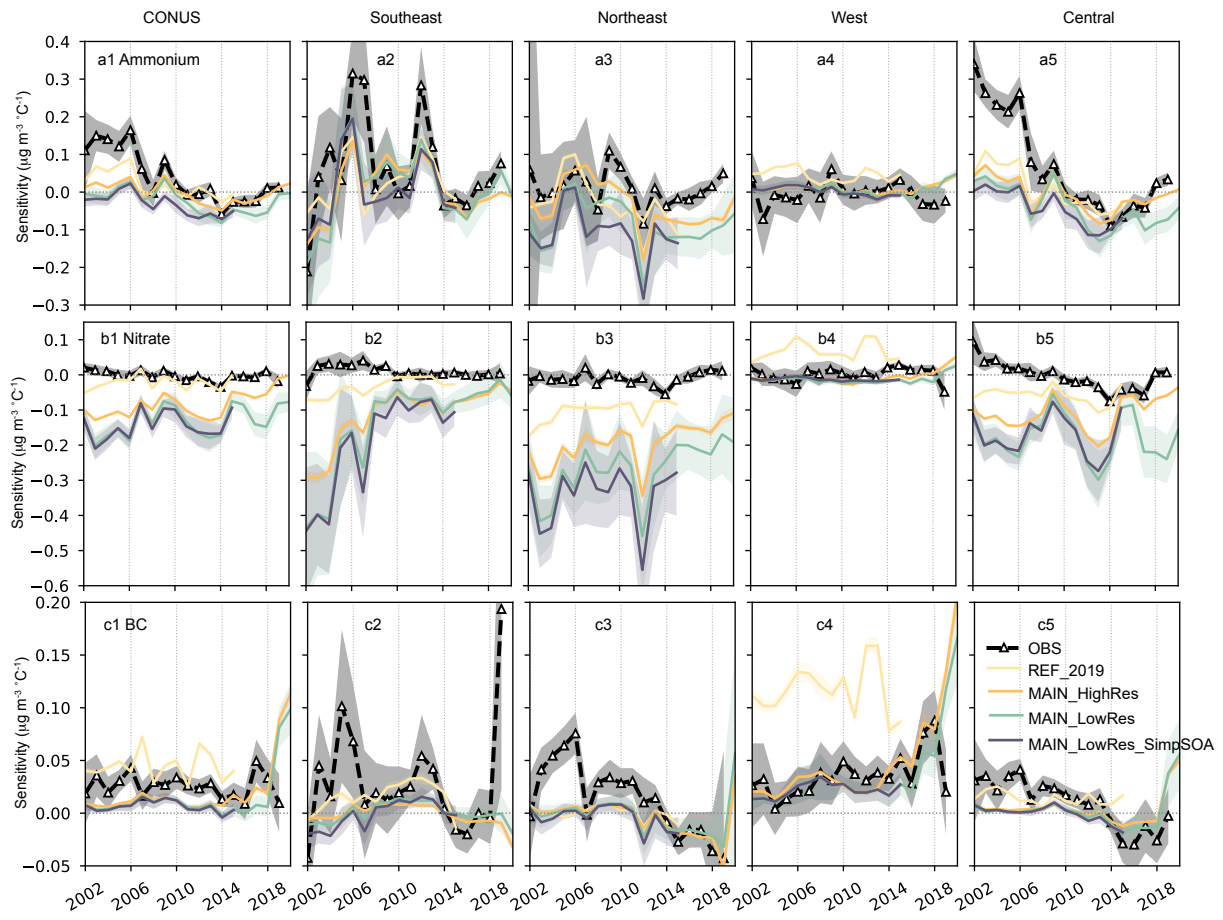


**Figure S12.** Same as Figure 2 in the main text, but for ammonium, nitrate, and black carbon (BC).

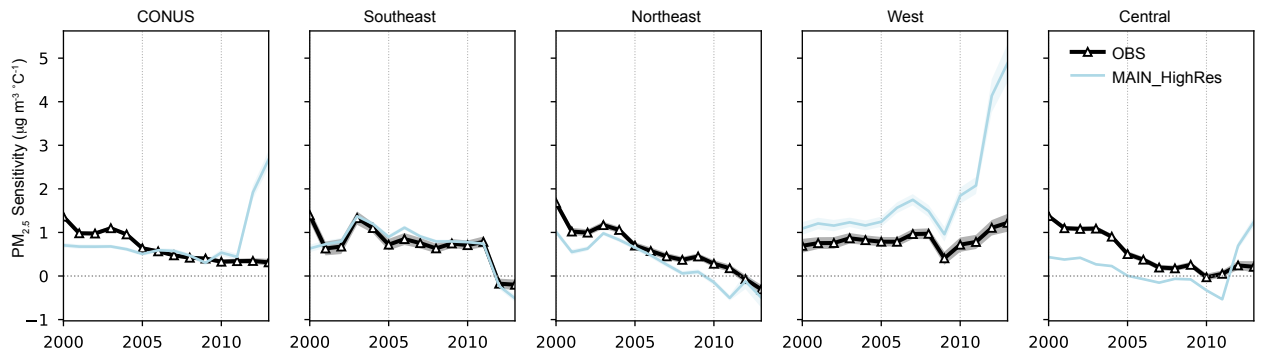


**Figure S13.** Regional-aggregated temperature sensitivity of PM<sub>2.5</sub> for 10-year running time windows, derived from ground-based observations and MAIN\_HighRes case. The shaded areas represent the 95% confidence interval across each region.

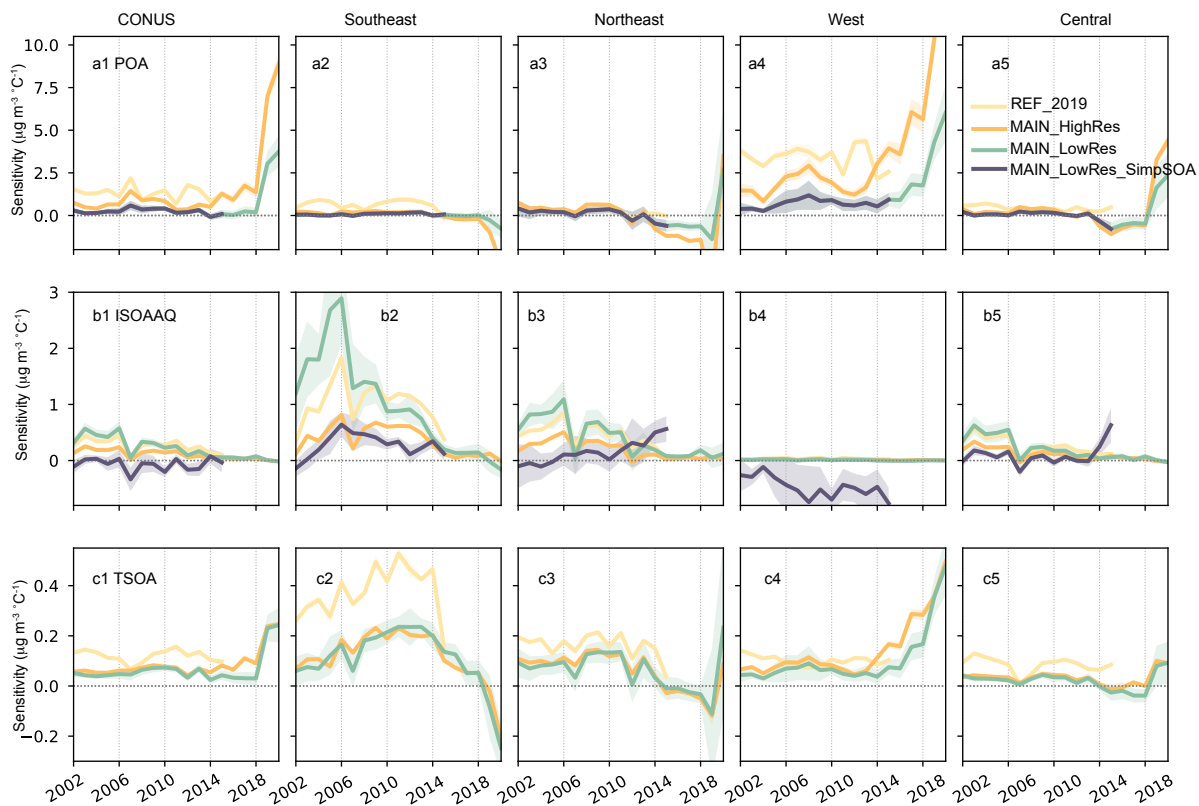


**Figure S14.** Regional-aggregated temperature sensitivity of three major organic aerosol (OA) species from four GEOS-Chem cases. Panels a1-a5 shows the temperature sensitivity of primary OA for the contiguous US (a1), the Southeast US (a2), the Northeast US (a3), the West US (a4), and the Central US (a5); Panels b1-b5 shows the temperature sensitivity of aqueous-phase formed isoprene OA (ISOAAQ) for each region; Panels c1-c5 shows the temperature sensitivity of monoterpene SOA (TSOA) for each region. The MAIN\_LowRes\_SimpSOA case reports total SOA concentrations as a single variable SOAS, which is shown with ISOAAQ in panels b1-b5.

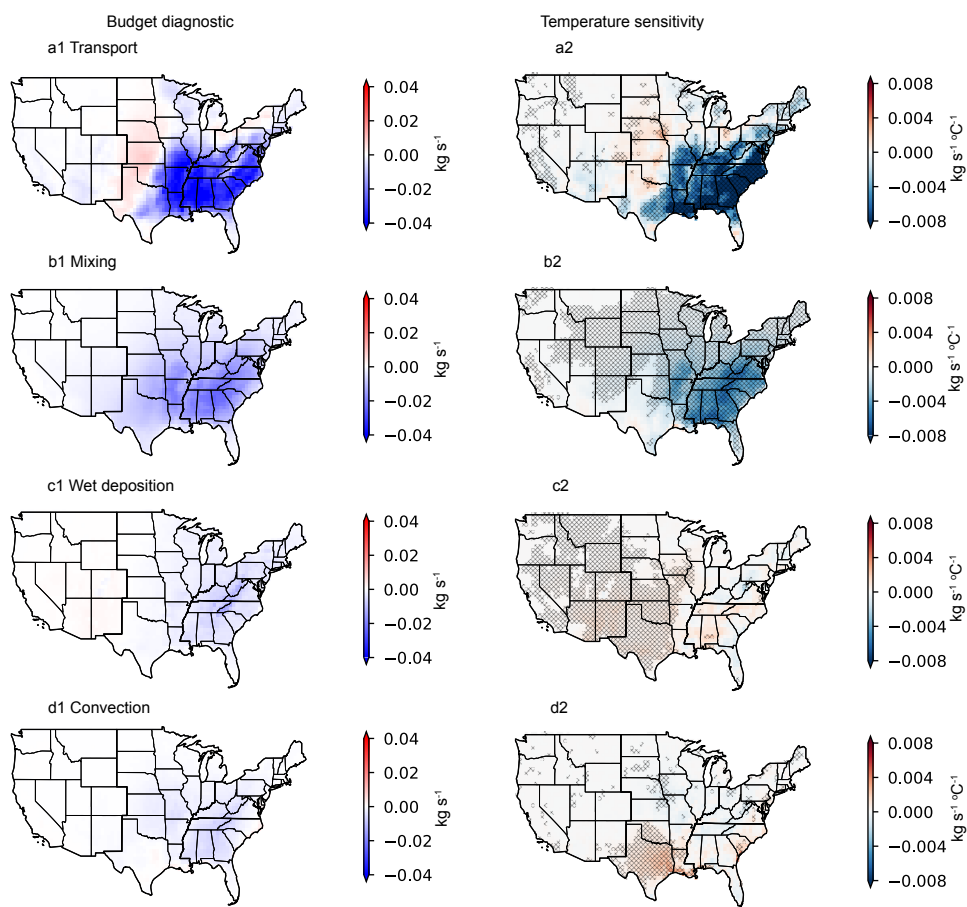


**Figure S15.** Budget diagnostic for aqueous-phase-formed isoprene SOA (ISOAAQ) simulated by the MAIN\_HighRes case and the temperature sensitivity of each process. Panels (a1–d1) show the budget diagnostic for transport (a1), mixing (b1), wet deposition (c1), and convection (d1) process and the corresponding temperature sensitivity (a2–d2).

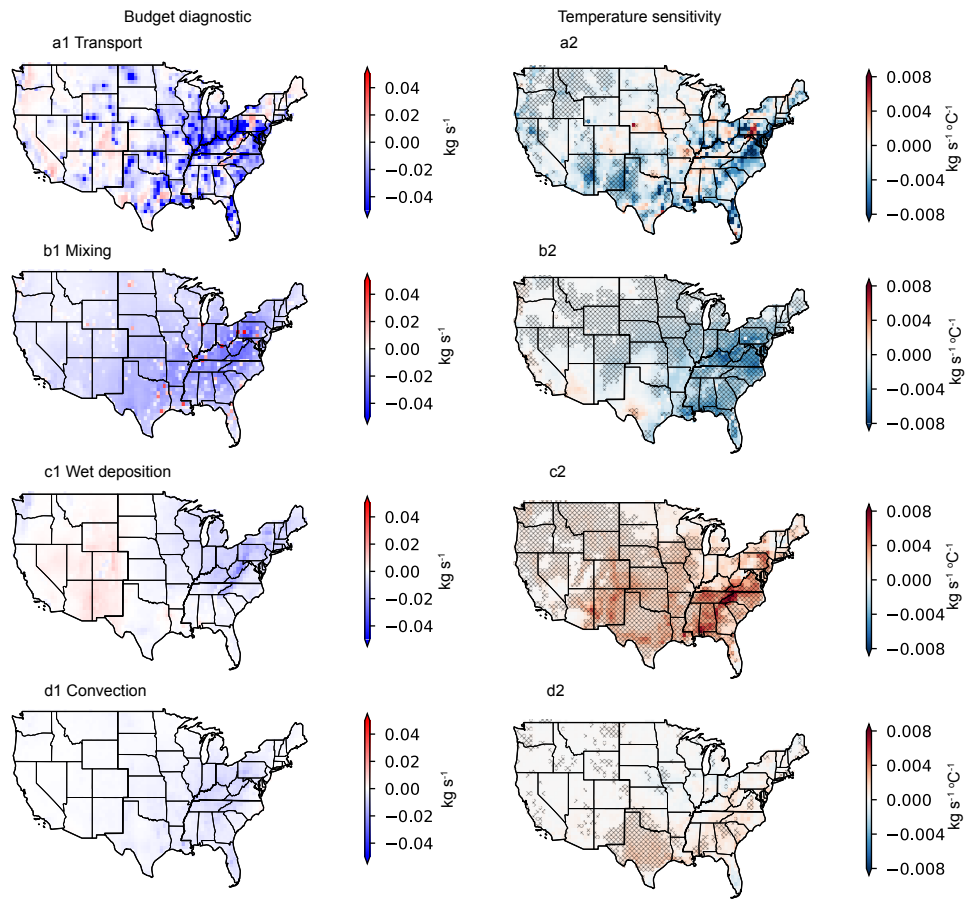


**Figure S16.** Same as Figure S15 but for sulfate budget diagnostic.

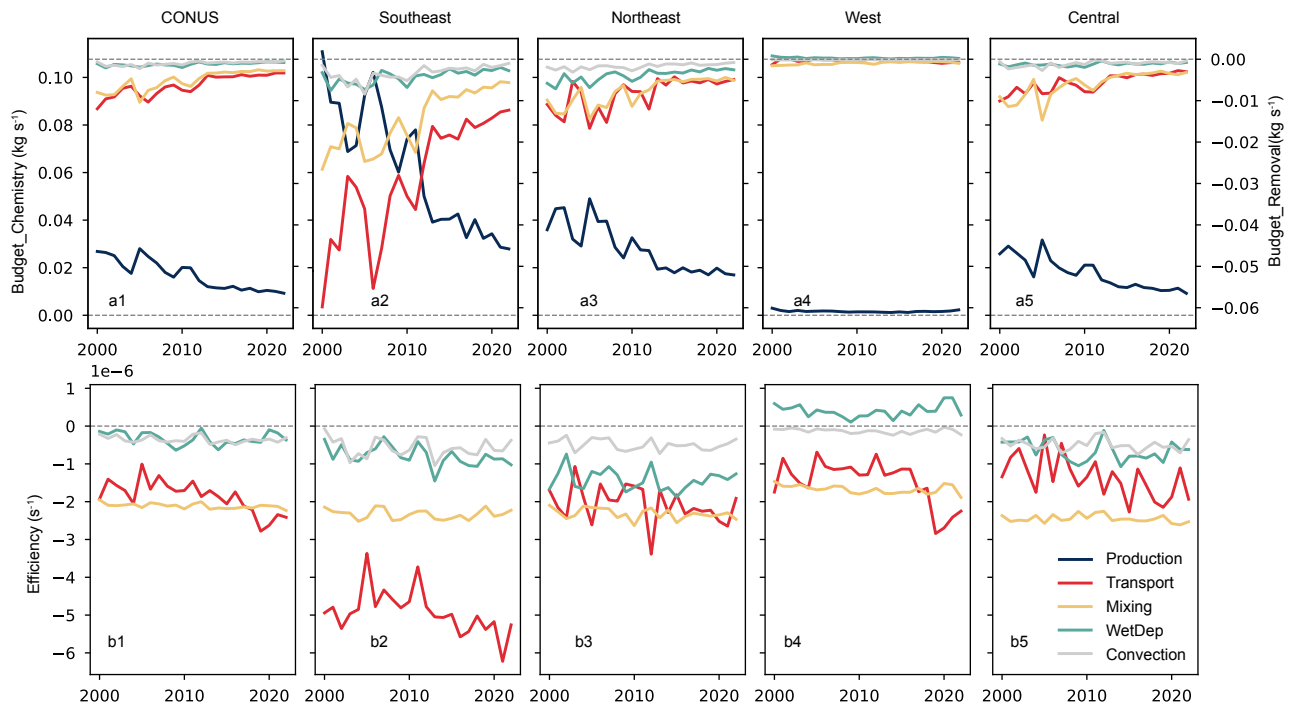


**Figure S17.** Time series for budget diagnostic and efficiency of driving processes of ISOAAQ concentration. Panels a1-a5 shows the time series for budget diagnostic for the contiguous US (a1), the Southeast US (a2), the Northeast US (a3), the West US (a4), and the Central US (a5); Panels b1-b5 shows the time series for removal efficiency for each region.

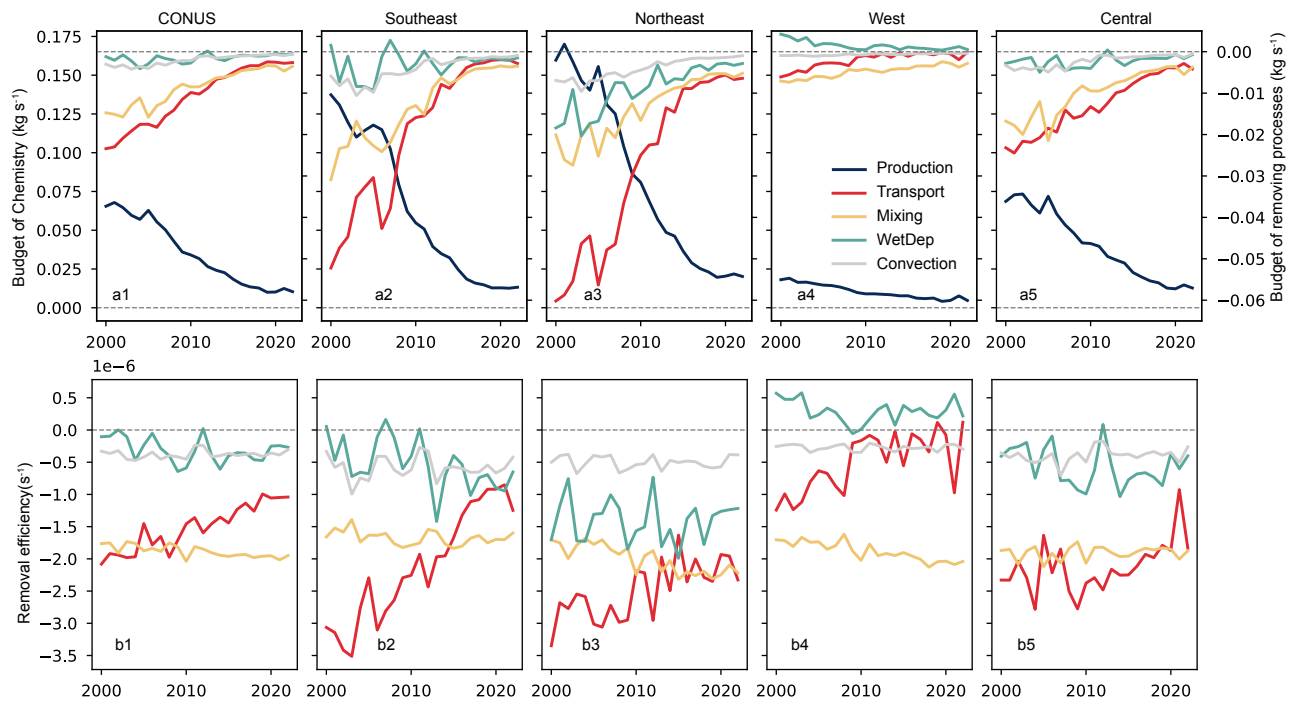


**Figure S18.** Same as Figure S17 but for sulfate budget diagnostic.

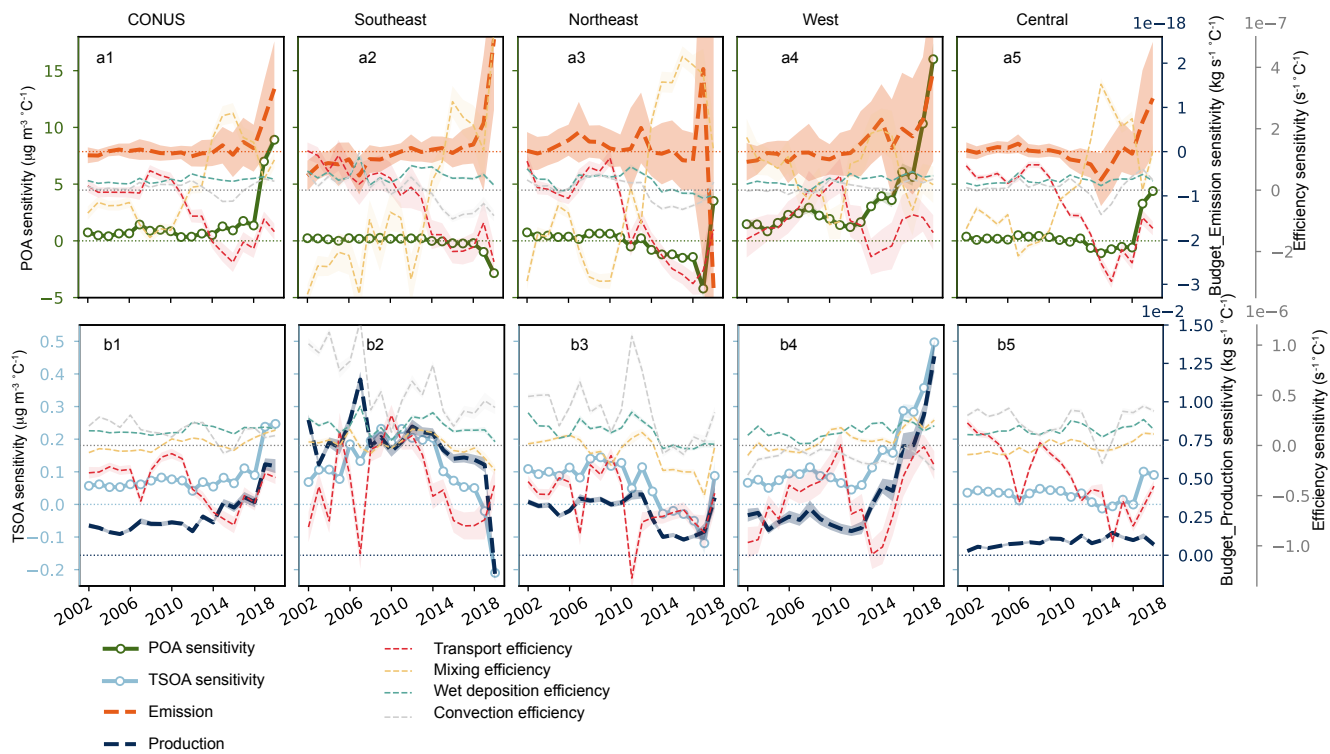


**Figure 19.** Same as Figure 5 in the main text but for primary organic aerosol (POA) and secondary organic aerosol formed from monoterpene oxidation (TSOA).

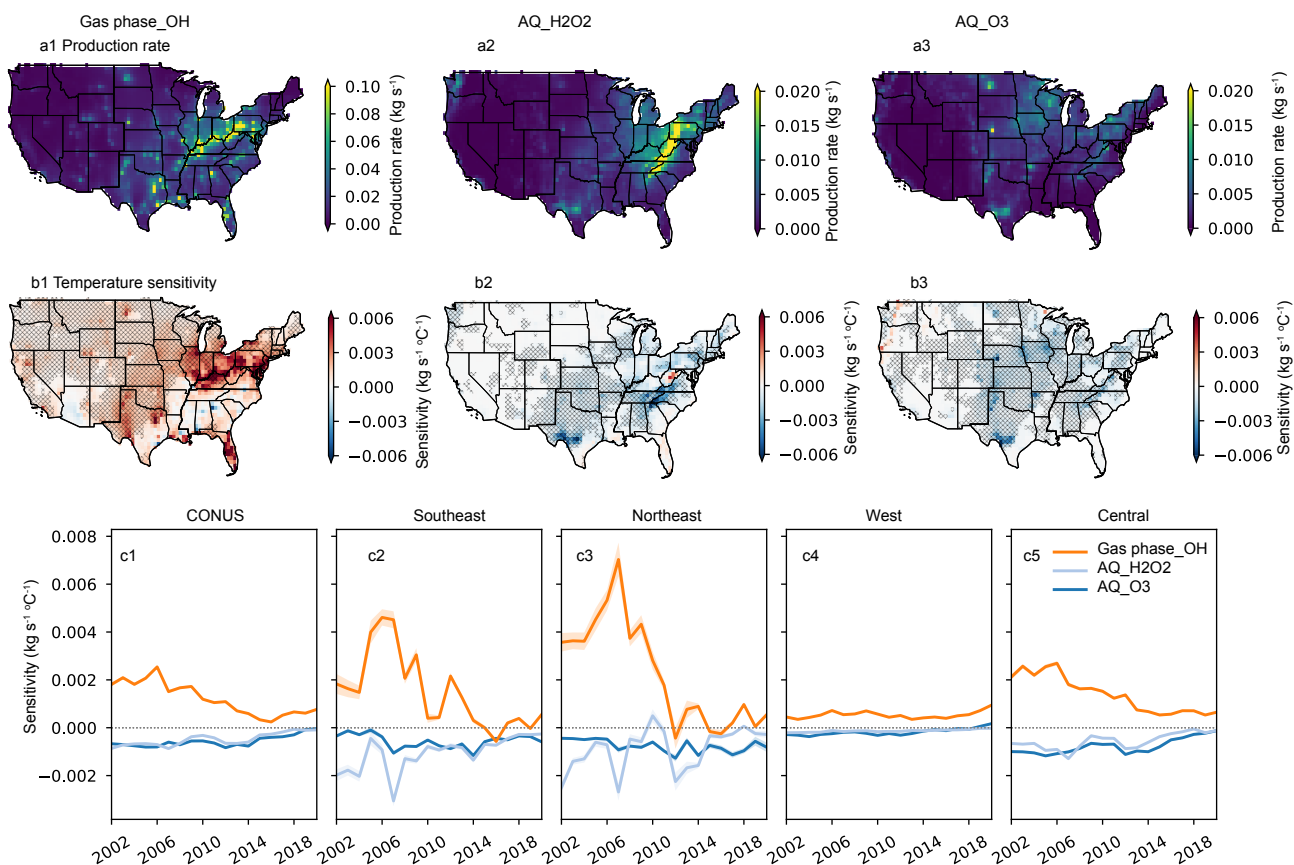


**Figure S20.** Production rate (a1-a3) and corresponding temperature sensitivity (b1-b3) of three major sulfate production processes. Panels c1-c5 shows the time series for temperature sensitivity of each pathway for the contiguous US (a1), the Southeast US (a2), the Northeast US (a3), the West US (a4), and the Central US (a5).

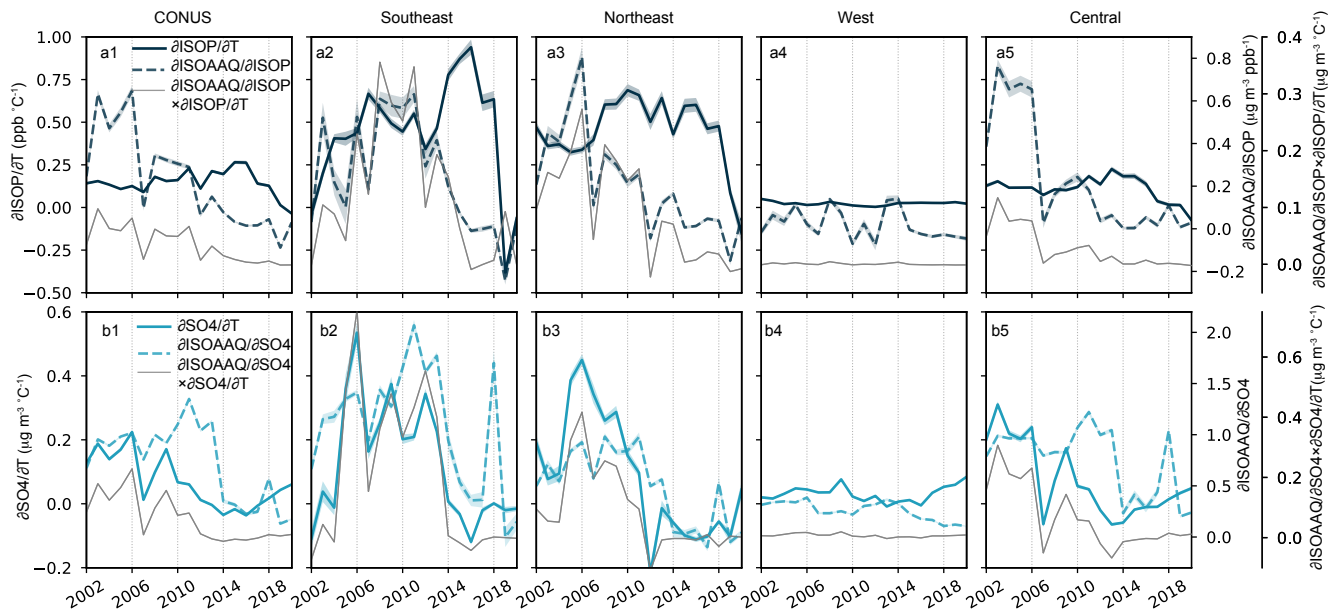


**Figure S21.** Contributions from isoprene-mediated and sulfate-mediated processes to the overall temperature sensitivity of isoprene SOA (ISOAAQ). The shading areas represent 95% confidence interval. Panels a1-a5 show the time series of isoprene-mediated process breakdown for the contiguous US (a1), Southeast US (a2), Northeast US (a3), West US (a4), and Central US (a5); Panels b1-b5 show the time series of sulfate-mediated process breakdown for each region. Please refer to Eq. (1) in the main text for detailed expression.

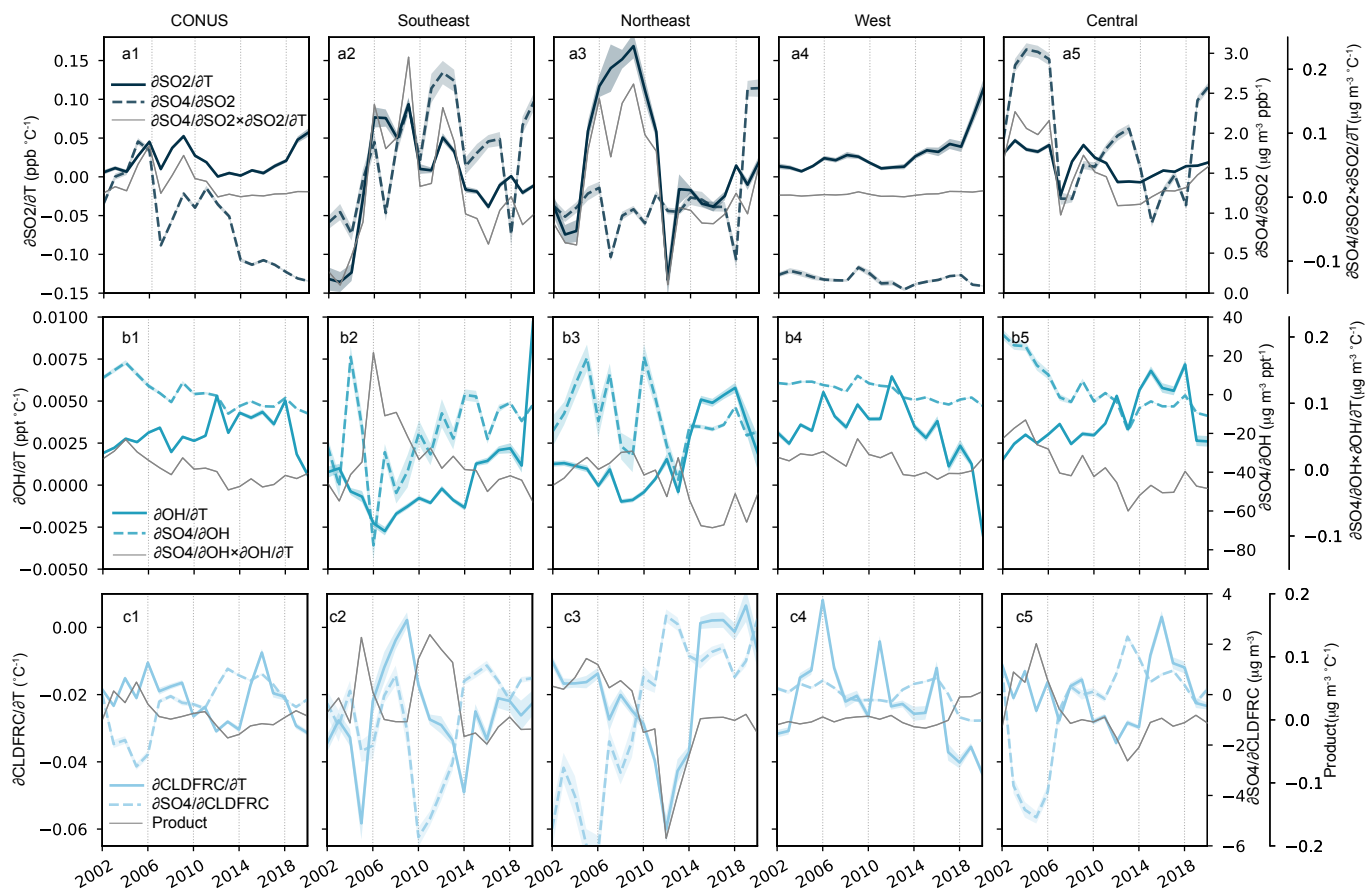


**Figure S22.** Same as Figure S21 but for sulfate. Please refer to Eq. (2) in the main text for detailed expression.

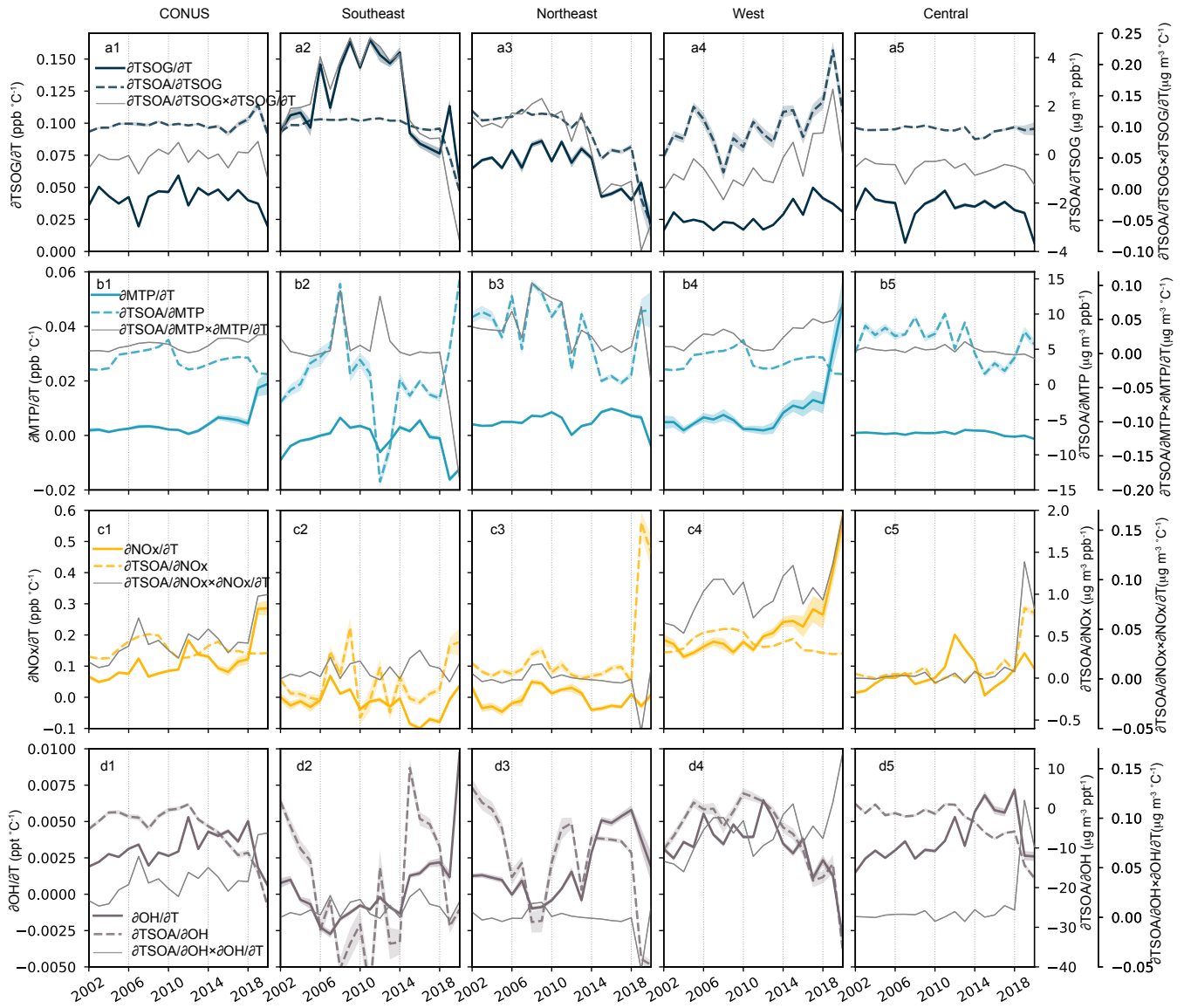


**Figure S23.** Same as Figure S21 but for monoterpene SOA (TSOA). Please refer to Eq. (3) in the main text for detailed expression.

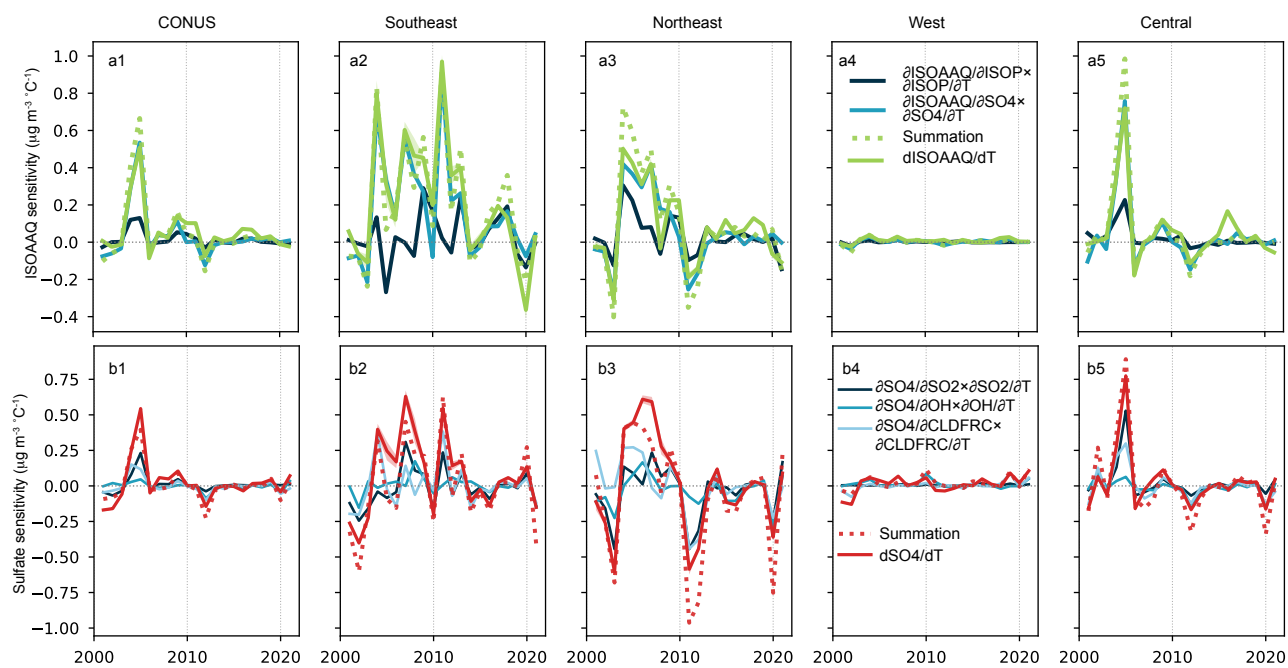


**Figure S24.** Same as Figure 6 a, b in the main text but for 3-year rolling window.

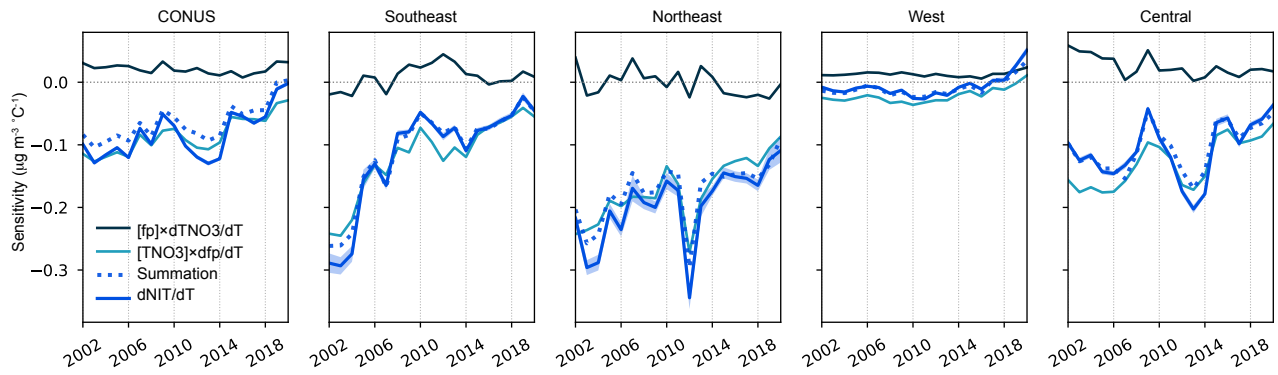


**Figure S25.** Same as Figure 6 in the main text but for nitrate aerosol. Please refer to Eq. (4) in the main text for detailed expression.